Light-activated resistance switching in SiO_x RRAM devices

A. Mehonic, T. Gerard, and A. J. Kenyon

Citation: Appl. Phys. Lett. **111**, 233502 (2017);
View online: https://doi.org/10.1063/1.5009069
View Table of Contents: http://aip.scitation.org/toc/apl/111/23
Published by the American Institute of Physics

Sharp, quick summaries illuminating
the latest physics research
Sign up for **FREE!**
AIP Publishing

APPLIED PHYSICS LETTERS **111**, 233502 (2017)

Light-activated resistance switching in SiO_x RRAM devices

A. Mehonic,[a)] T. Gerard,[a)] and A. J. Kenyon
Department of Electronic & Electrical Engineering, UCL, Torrington Place, London WC1E 7JE, United Kingdom

(Received 12 October 2017; accepted 20 November 2017; published online 4 December 2017)

We report a study of light-activated resistance switching in silicon oxide (SiO_x) resistive random access memory (RRAM) devices. Our devices had an indium tin oxide/SiO_x/p-Si Metal/Oxide/Semiconductor structure, with resistance switching taking place in a 35 nm thick SiO_x layer. The optical activity of the devices was investigated by characterising them in a range of voltage and light conditions. Devices respond to illumination at wavelengths in the range of 410–650 nm but are unresponsive at 1152 nm, suggesting that photons are absorbed by the bottom p-type silicon electrode and that generation of free carriers underpins optical activity. Applied light causes charging of devices in the high resistance state (HRS), photocurrent in the low resistance state (LRS), and lowering of the set voltage (required to go from the HRS to LRS) and can be used in conjunction with a voltage bias to trigger switching from the HRS to the LRS. We demonstrate negative correlation between set voltage and applied laser power using a 632.8 nm laser source. We propose that, under illumination, increased electron injection and hence a higher rate of creation of Frenkel pairs in the oxide—precursors for the formation of conductive oxygen vacancy filaments—reduce switching voltages. Our results open up the possibility of light-triggered RRAM devices. © *2017 Author(s). All article content, except where otherwise noted, is licensed under a Creative Commons Attribution (CC BY) license (http://creativecommons.org/licenses/by/4.0/).*
https://doi.org/10.1063/1.5009069

Recent years have seen great interest in emerging memory technologies, with resistive random access memory (RRAM)[1] being one of the most promising candidates, with low power consumption, high speed switching, and high density storage in 3D arrays demonstrated.[2,3] Two-terminal resistance switching elements can change resistance under an appropriate voltage bias. The ability to retain the last resistance state even without a voltage bias suggests a range of potential applications including non-volatile memories,[4] logic,[5] and unconventional computing architectures.[6–8] In filamentary resistance switching, the resistance change is governed by formation and annihilation of conductive filaments inside initially insulating layers—typically metal binary oxides and perovskites. In the case of intrinsic filamentary resistance switching, in which changes in resistance are driven by changes to the structure of the oxide matrix rather than by indiffusion of metal ions from one of the electrodes (extrinsic switching), the filaments are generally considered as chains of oxygen vacancies, generated by the field-driven rearrangement of oxygen within the oxide. Resistance transitions are achieved by the application of voltage biases across metal-insulator-metal (MIM) structures, which drives the movement of oxygen ions. A crucial first step in this process is the generation of mobile oxygen species which, in the case of silicon oxide, is thought to involve a combination of applied field and electron injection.[9,10] There have been a handful of studies on light controllable resistance switching,[11–14] which conclude that optical illumination can improve switching properties or be an enabler for resistance switching. In these studies, the light illumination was used to control the resistance by modulating the trapped electrons in the binary strucutres[11] or by modulating the Schottky-like barriers.[12] Other approaches include the use of the intrinsic photoconductivity of 1D metal oxide nanorods[13] and the use of photoferroelectric effects in multiferroic materials.[14] Here, we report that the use of an optically active p-type silicon electrode provides an additional control method, beyond the applied field, in resistance switching of silicon oxide RRAM devices. More specifically, we observe a decrease of the set voltage [required to switch from the high resistance state (HRS) to the low resistance state (LRS)] by applying light within the visible spectrum. Furthermore, distinctively to studies mentioned above, we demonstrate that it is possible to set devices optically in conjunction with a voltage bias that is too low to initiate switching on its own.

The RRAM devices used in this experiment had a metal-oxide-semiconductor (MOS) structure. They were fabricated by depositing 35 nm of silicon oxide onto p-type, B-doped Si(100) wafers by magnetron co-sputtering at 500 °C. The silicon oxide was measured to have an excess silicon content of 11%, as measured by XPS (Perkin-Elmer PHI-5500). This gives the SiO_x stoichiometry close to $x \sim 1.3$. In our previous study, we found that the oxide layer is rich in asymmetrical $SiO_2{\equiv}Si–Si$ and $O_3{\equiv}Si–Si$ configurations.[15] After deposition, the samples were annealed at 500 °C under nitrogen for one hour. Once cooled, 70 nm of indium tin oxide (ITO) was deposited on top of the silicon oxide by sputtering. 500 μm × 500 μm square contacts were defined by standard photolithography followed by a 30 s bath in hydrochloric acid. A chrome-gold Ohmic contact was applied to the base of the silicon substrate by evaporation. This consisted of 10 nm of

[a)]A. Mehonic and T. Gerard contributed equally to this work.

 © Author(s) 2017.

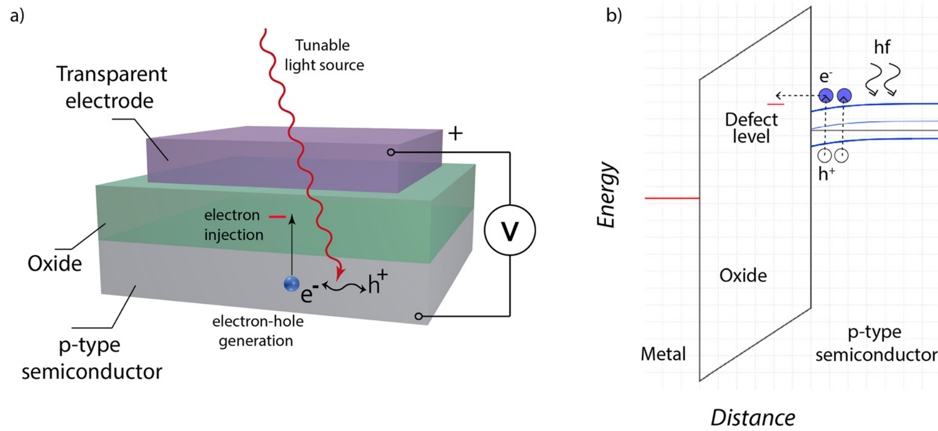

FIG. 1. (a) The MOS (metal-oxide-semiconductor) structure consisting of a transparent top electrode (ITO), thin silicon oxide layer (35 nm), and bottom p-type Si substrate. A light source is introduced during the electrical stimuli to generate electron-hole pairs in the substrate. (b) Corresponding energy band diagram. Minority carriers are optically generated in the p-type substrate and are injected into the oxide layer by the applied field.

chrome and 100 nm of gold. We found that the oxides in the range of 30–40 nm give the best switching properties. A schematic of the device and the experimental setup is shown in Fig. 1(a).

Electrical measurements were performed using a Keithley 4200 Semiconductor Characterisation System and a Signatone probe station. Testing was performed at room temperature within a dark box. Light was introduced to the RRAM device via a fibre optic bundle attached to an optical microscope. Five different laser sources were used, with wavelengths spanning the visible and near infra-red, as well as white light from a tungsten filament bulb.

A summary of the laser powers incident on the sample for different source wavelengths is detailed in Table I.

Figure 2(a) shows a typical current-voltage switching curve of the RRAM device in darkness after electroforming. By raising the voltage above a threshold voltage V_{SET}, the device transitions from the high resistance state (HRS) to the low resistance state (LRS)—the set process [steps (i) to (iii)]. The device remains in the LRS until a negative threshold V_{RESET} is achieved. At this point, the device switches back to the HRS (the reset process), as shown in steps (iv) to (vi). More details about electrical performance and switching mechanisms in SiO_x are given in our previous reports.[16–20] We note that the devices typically operate better in ambient rather than vacuum conditions. Similar behaviour has been reported by other groups as well.[21] In particular, the reset process is harder to achieve in vacuum. This could be due to the lack of environmental oxygen necessary for the re-oxidation of filaments or more extreme loss of oxygen during the electroforming process. We found that the devices are stable at elevated temperatures.[16,18]

TABLE I. The list of laser sources used. Source power, P, experiences attenuation and spread by being directed through a fibre optic bundle and optical microscope. The actual power reaching the RRAM device is given by P_{RRAM}.

Source	Wavelength (nm)	P (mW)	P_{RRAM} (μW)
632.8	632.8 ± 0.1	0.65 ± 0.03	0.04 ± 0.01
650	650 ± 10	2.2 ± 0.1	0.14 ± 0.03
532	532 ± 10	9.2 ± 0.7	0.6 ± 0.1
410	410 ± 10	12 ± 2	0.8 ± 0.3
1152	1152 ± 1	0.48 ± 0.05	0.03 ± 0.01

To characterise the response to optical stimulation, the device was put in the HRS and biased with a constant voltage. Current was sampled every 0.3 s for 15 s. The device was exposed to white light for the central 5 s (orange in Fig. 2). This was repeated for a range of applied voltages [Figs. 2(b)–2(e)]. Four different responses are observed depending on the initial resistance state and the bias voltage. In the HRS and at low bias voltage (1 V), Fig. 2(b) shows little response to the light. At 4 V, current spikes and decays are observed at the leading and trailing edges of the light pulse [Fig. 2(c)]. This is a typical capacitor charging and discharging response due to the generation of excess carriers in the system, which flow in the external circuit. This indicates that no conductive filaments are formed at this point. At 5 V, the device shows an abrupt jump in current when exposed to light. The current level remains high even after the removal of the light, demonstrating a set transition [Fig. 2(d)]. This is evidence of light-triggered switching. The sub-threshold switching voltage can vary from device to device and from cycle to cycle; it is related to the inherent variability of switching voltages in RRAM devices which, while rather large in this non-optimised device, can be greatly reduced through appropriate material and device design.[17,19] Finally, Fig. 2(e) shows the device response in the LRS; current rises and falls when exposed to light. This is typical of a photo-induced transient current without a permanent conduction change.

We analysed how the wavelength of the laser affects resistance switching. Time-bias measurements were performed on devices in the HRS at a bias of 5 V while exposing them to five different laser sources (Table I). The 1152 nm laser light does not induce any response, indicating that photons of this wavelength have insufficient energy to generate photocarriers. This supports the hypothesis that light is absorbed in the silicon bottom electrode, as the photon energy of 1.08 eV is smaller than the bandgap of silicon at room temperature (1.12 eV). The response of devices to laser wavelengths within the visible spectrum is shown in Figs. 3(a)–3(d).

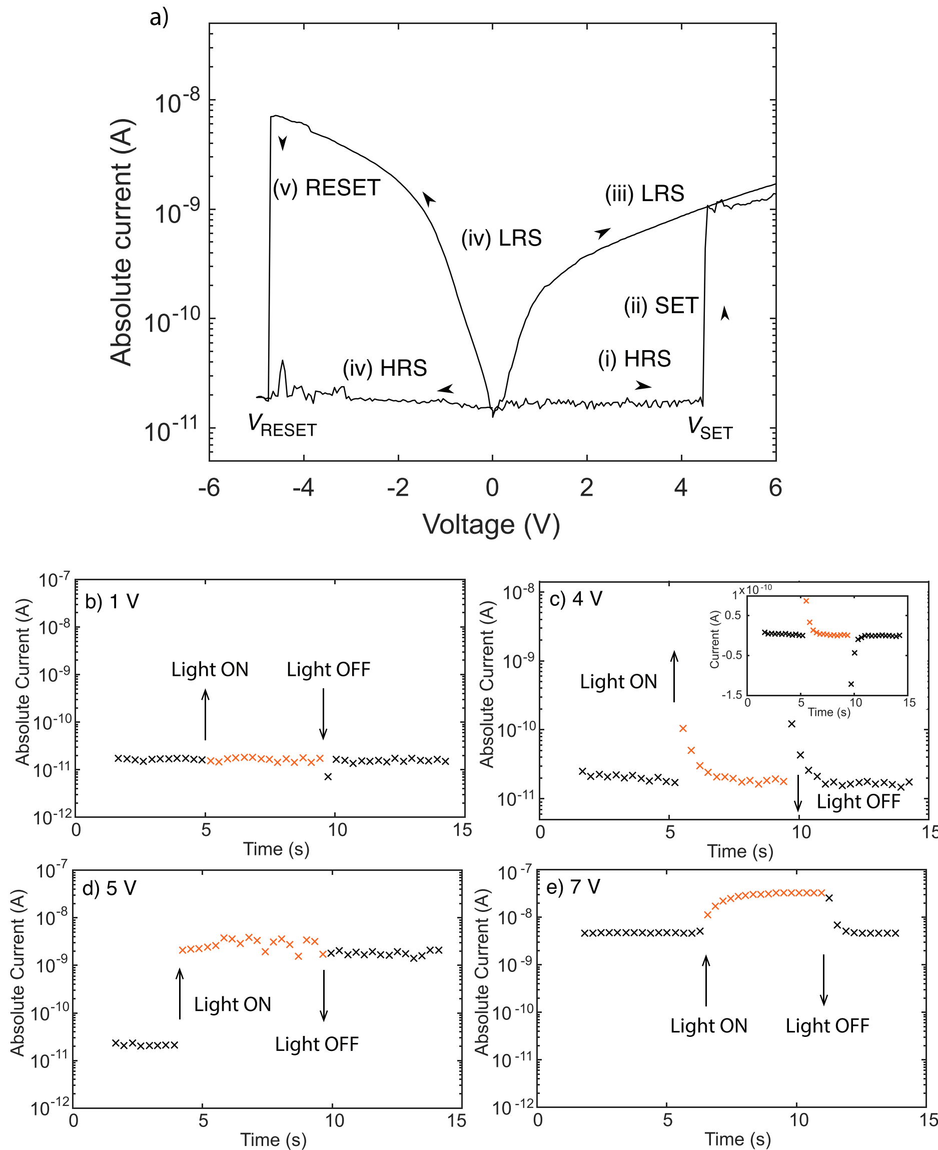

FIG. 2. (a) Typical current-voltage switching curves. (b)–(e) show the device's response to white light at different voltages. For low bias voltages, (b), light has little effect. At higher voltages, (c) a typical capacitor-like response is observed in which charging and discharging currents flow in the external circuit. The inset of (c) shows the response plotted on a linear scale: current flows in alternate polarities as the light is switched on and off. At 5 V (d), which is insufficient to switch the device in the dark, the device switches from the HRS into the LRS with the application of light. It remains in this state when the light is switched off. (e) When in the LRS, light causes an increase in current that returns to its initial levels once the light is removed.

To characterise the effect of the laser power on V_{SET}, the 632.8 nm laser was directed through neutral density filters to vary the incident optical power. Repeated voltage sweeps of 0–10 V were performed and V_{SET} measured. Devices were reset between sweeps. The mean and standard error on the mean of V_{SET} were calculated. 131 sweeps were performed in darkness, and 62 under full power (41 nW). 25 sweeps were performed for all other incident powers. The decrease of V_{SET} with incident laser power is shown in Fig. 3(e). Lastly, once the device is set into the LRS, we observe that photocurrent varies with the applied wavelength. A responsivity curve can was therefore constructed by comparing photocurrent to normalised laser power at different wavelengths [Fig. 3(f)]. The most significant source of uncertainty is the attenuation experienced by the light when passed through the fibre optic bundle and optical microscope, adding a baseline uncertainty of 15% to all visible wavelength sources. The responsivity results are compared to the responsivity curve of a typical silicon photodiode decreased by a factor of 10 [Fig. 3(f)]. The RRAM responsivity data follow the photodiode curve, falling off after 1000 nm, justifying the p-type silicon substrate as the optically active element of the device. Note that MIM structures with metallic top and bottom electrodes do not exhibit light-induced activity, further confirming that photon absorption occurs in the silicon bottom electrode.

Several potential effects may lower V_{set} as well as produce light-activated settings. Previous reports from oxide films suggested that trapping and detrapping of optically generated charges at a Schottky-like barrier could be responsible for the differences in device behaviour in the dark and under illumination.[11,12] However, we note that in our devices, the dominant conduction mechanism is trap-assisted tunnelling,[16] and therefore, we suggest a different mechanism.

We propose that that the generation of electron-hole pairs by incident light enhances electron injection from the silicon electrode into pristine trap sites in the silicon oxide under electrical bias. This is a crucial first step in the generation of mobile oxygen species in SiO_x. Electron injection and trapping at intrinsic defects in the pristine oxide lead to the increase in the creation rate of Frenkel pairs, which consist of oxygen vacancies and oxygen interstitial ions,

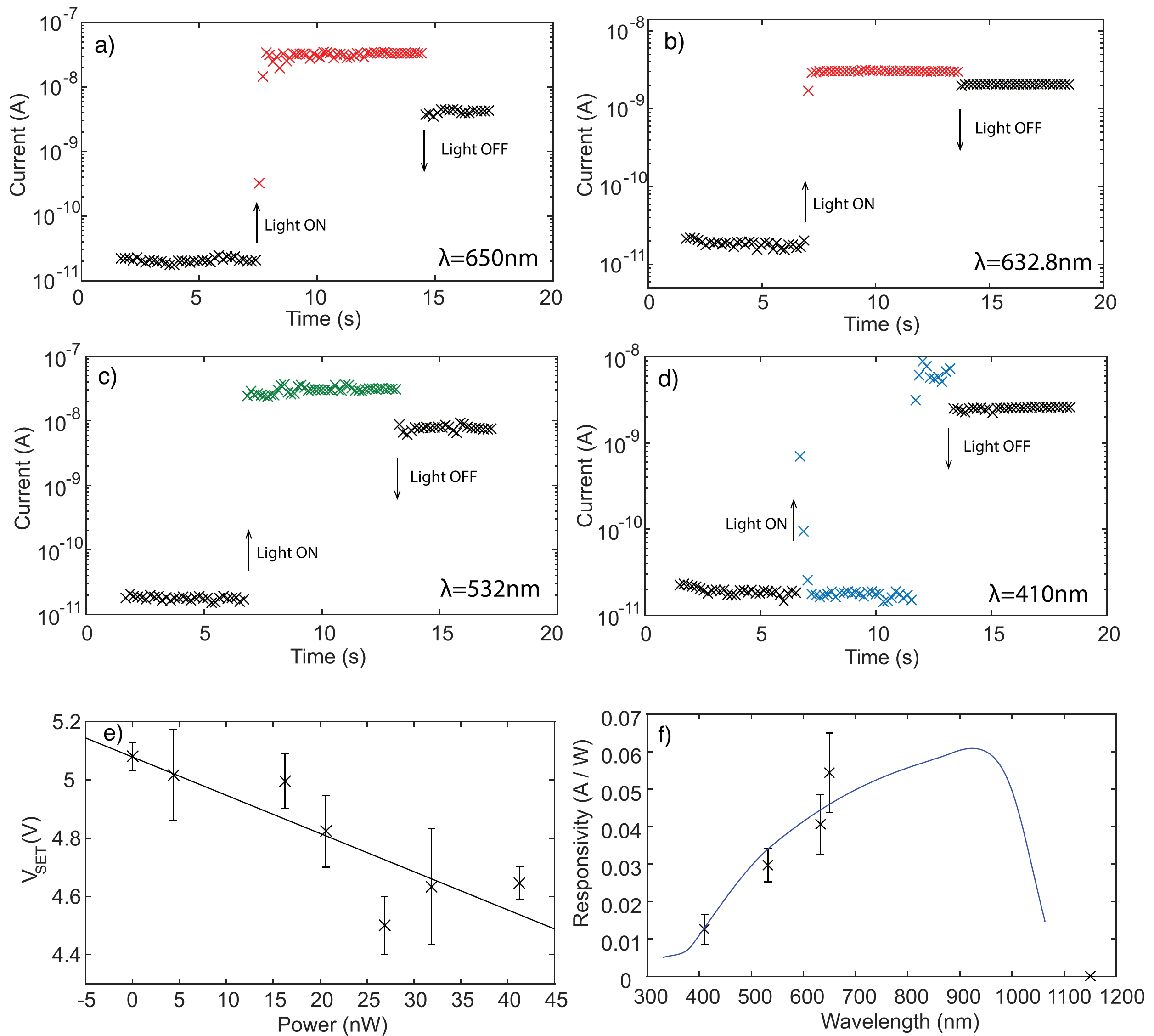

FIG. 3. Light-triggered switching at different wavelengths (a)–(d). No light-triggered switching was observed when exposing the device to 1152 nm light. (e) Mean set voltage V_{SET} variation with applied power at 632.8 nm. Each data point is an average of 25 V_{SET} measurements. Note that the shown error bars are the standard error on the mean. (f) Variation in induced photocurrent with laser wavelength for the LRS. A typical silicon photodiode responsivity curve reduced by a factor of 10 is overlaid for comparison.

with oxygen interstitial ions having low migration barriers (around 0.2 eV).[9,22] This results in faster conductive filament production by promoting oxygen vacancy formation. Once sufficient vacancies have been generated to create a continuous or semi-continuous filament bridging the oxide, the device switches to the LRS. The evidence of the filamentary switching can be found in our previous study.[19] Here, we have used the conductive atomic force microscopy (CAFM) tomography to study the nature of the resistance switching by localising and reconstructing the 3 D images of the conductive filaments. Further, we have been able to modulate the conduction of localised areas by applying the bias to scanning tunnelling microscope (STM) tips.[17] The combination of the low applied electric field with the generation of excess carriers by optical illumination enables us to separate the contributions of the applied field and carrier injection; our results support the hypothesis from Ref. 9 that electron injection, not field, is the rate limiting step in Si-O bond breakage, formation of Frenkel pairs, and generation of conductive filaments. Our results further enable an added mode of operation for SiO_x RRAM devices—optical triggering.

In summary, the optical activity of RRAM devices was investigated by characterising ITO/silicon oxide/p-type-silicon devices in a range of voltage and optical conditions. Using broadband white light and red, green, blue, and infrared laser light, the RRAM devices were shown to be optically active under all but infrared laser light. This optical activity was demonstrated to cause charging across the RRAM device in the HRS and photocurrent in the LRS and could be used to switch the device from the HRS to the LRS in conjunction with a voltage bias. The lack of response to photons with energy smaller than the silicon bandgap confirmed the silicon substrate as the optically active region of the device. We hypothesise that enhancement of electron injection into

traps in the pristine oxide layer and subsequent generation of Frenkel pairs promote the formation of conductive filaments of oxygen vacancies.

We gratefully acknowledge funding provided by EPSRC under Grant No. EP/P013503/1 "Structural dynamics of amorphous functional oxides—the role of morphology and electrical stress" and by RAEng under the Research Fellowship "Next Generation Adaptive Electronics for Neuromorphic Engineering."

[1]R. Waser and M. Aono, Nat. Mater. **6**(11), 833 (2007).
[2]A. C. Torrezan, J. P. Strachan, G. Medeiros-Ribeiro, and R. S. Williams, Nanotechnology **22**(48), 485203 (2011).
[3]H. Y. Chen, S. Yu, B. Gao, P. Huang, J. Kang, and H.-S. P. Wong, in *IEEE International Electron Device Meeting (IEDM)* (2012), pp. 20.7.1-20.7.4.
[4]R. Waser, R. Dittmann, G. Staikov, and K. Szot, Adv. Mater. **21**, 2632 (2009).
[5]J. Borghetti, G. S. Snider, P. J. Kuekes, J. J. Yang, D. R. Stewart, and R. S. Williams, Nature **464**(7290), 873 (2010).
[6]S. H. Jo, T. Chang, I. Ebong, B. B. Bhadviya, P. Mazumder, and W. Lu, Nano Lett. **10**(4), 1297 (2010).
[7]A. Serb, J. Bill, A. Khiat, R. Berdan, R. Legenstein, and T. Prodromakis, Nat. Commun. **29**(7), 12611 (2016).
[8]A. Mehonic and A. J. Kenyon, Front. Neurosci. **10**, 57 (2016).
[9]D. Gao, A. El-Sayed, and A. L. Shluger, Nanotechnology **27**, 505207 (2016).
[10]A. Padovani, D. Z. Gao, A. L. Shluger, and L. Larcher, J. Appl. Phys. **121**(15), 155101 (2017).
[11]M. Ungureanu, R. Zazpe, F. Golmar, P. Stoliar, R. Llopis, F. Casanova, and L. E. Hueso, Adv. Mater. **24**(18), 2496 (2012).
[12]B. Sun, J. Wu, X. Jia, F. Lou, and P. Chen, J. Sol-Gel Sci. Technol. **75**(3), 664 (2015).
[13]J. Park, S. Lee, and K. Yong, Nanotechnology **23**(38), 385707 (2012).
[14]B. Sun, Y. Liu, W. Zhao, and P. Chen, RSC Adv. **5**(18), 13513 (2015).
[15]A. Mehonic, M. Buckwell, L. Montesi, L. Garnett, S. Hudziak, S. Fearn, R. Chater, D. McPhail, and A. J. Kenyon, J. Appl. Phys. **117**, 124505 (2015).
[16]A. Mehonic, S. Cueff, M. Wojdak, S. Hudziak, O. Jambois, C. Labbe, B. Garrido, R. Rizk, and A. J. Kenyon, J. Appl. Phys. **111**, 074507 (2012).
[17]A. Mehonic, S. Cueff, M. Wojdak, S. Hudziak, C. Labbé, R. Rizk, and A. J. Kenyon, Nanotechnology **23**, 455201 (2012).
[18]A. Mehonic, M. S. Munde, W. H. Ng, M. Buckwell, L. Montesi, M. Bosman, A. L. Shluger, and A. J. Kenyon, Microelectron. Eng. **178**, 98 (2017).
[19]M. Buckwell, L. Montesi, S. Hudziak, A. Mehonic, and A. J. Kenyon, Nanoscale **7**, 18030 (2015).
[20]M. S. Munde, A. Mehonic, W. H. Ng, M. Buckwell, L. Montesi, M. Bosman, A. L. Shluger, and A. J. Kenyon, Sci. Rep. **7**, 9274 (2017).
[21]Y. Wang, X. Qian, K. Chen, Z. Fang, W. Li, and J. Xu, Appl. Phys. Lett. **102**, 042103 (2013).
[22]A. Mehonic, M. Buckwell, L. Montesi, M. S. Munde, D. Z. Gao, S. Hudziak, R. J. Chater, S. Fearn, D. McPhail, M. Bosman, A. L. Shluger, and A. J. Kenyon, Adv. Mater. **28**, 7486 (2016).